Detached-Eddy Simulation of Massively Separated Flows around Airfoil

Li Dong, Igor Men'shov, and Yoshiaki Nakamura (Nagoya University)

Abstract: Detached-Eddy Simulation is applied to three airfoils with different stall types. The method combines the strong points of Reynolds-averaged Navier-Stokes and Large Eddy Simulation approaches. Spalart-Allmaras Model is basically used, which reduces to a RANS formulation near a solid surface and to a subgrid model away from the wall. LU-SGS implicit scheme is employed to solve the model in time. Compared with experiment data, it is found that stall angle can be reasonably predicted by the present method.

Key word: Detached-Eddy Simulation, Airfoil stall, Spalart-Allmaras turbulence model

Introduction

In the massive three-dimensional separation zones typical for vehicles and airplane components, Reynolds Average NS (RANS) turbulence models meet it's limitations because the dominant "detached" eddies in massively separated flows are highly geometry-specific which has little to do with the fairly universal turbulence-model calibration [1](M,Strelets). On the other hand, recent estimates for the cost of Large Eddy Simulation (LES) of an airplane [2] (Spalart,P.R) show that due to the presence of thin near-wall turbulent boundary layers populated with small "attached" eddies whose local size is much less than the boundary layer thickness, that the cost exceeds the available computing power by orders of magnitude. As a result, there is no real prospect of using LES in complex engineering computations for a very long time.

To fit the need of the computation of massively separated turbulent flows in practical geometries at practice Reynolds numbers, Spalart et.al. [3] proposed Detached-Eddy Simulation (DES) with the objective of developing a numerically feasible and accurate approach combining the most favourable elements of RANS models and LES. The primary advantage of DES is that it can be applied at high Reynolds numbers as can RANS techniques, and also resolves geometry dependent unsteady three-dimensional turbulent motions as in LES.

DES technique has been used for delta wing vortex breakdown [4](Scolt Morton), supersonic axisymmetric base flow [5](James R.Forsythe), circular cylinder, rounder square, airfoil pitch-up, real configuration of several aircraft [6](Kyle D.Squires) and so on. It is noticeable that all the simulation works are focus on the practice Reynolds numbers for aviation case. By the numerical experience for Delta wing [4], DES results are compared with the RANS results, although RANS results with turbulence model and with rotation correct give well prediction for vortex breakdown as DES methods, it didn't show the hope of improving with a refinement in grid as is the case with DES method, which is a important figure of LES methods. For the supersonic axisymmetric base simulation, both boundary layer on the body and wake separated flow in the base region are predicted by DES [6]. Smoothly transition from RANS region to LES region are observed in DES flow field, and it return to RANS approach when flow field is attached, means that the benefit of RANS known to be most adequate in terms of computational cost, robustness and credibility remains. As practice use for fighter aircraft at high attack angle by DES [7](James R.Forsythe), three different densities of grids is used for the test to compare the RANS results and DES results. DES gives better simulation for lift at every lever of grids, and, the most important things is that, as the refinement of grid, lift accuracy was improved by DES, which is not observed in RANS results. As shown in reference, current computation condition is available for the practice use of aviation massive separation problem by using DES methods. For the axisymmetric base flow, with 4.5E6 Reynolds numbles, and 2.75 million grids points, by 256 processor, 30 wall clock hours is cost [5]. And for a real configuration of aircraft using 3 million grid points, by using 432SP3 processors, 12.5 hours give an acceptable result. Ever with a fine grid with 10 million grid points, by 256 processor, four days calculation give a results within 5% of the flight-test data [5]. As a conclusion, DES method is a practice method for massive separated flow for aviation engineering.

Current research work is a response to the CFD workshop on "airfoil stall prediction" proposed by National Aerospace Lab (NAL) of Japan. Results from several teams in Japan had been

published to answer this question [8] Although for the case before stall, almost all paper give quite good results, it is found that it is difficult to predict the stall angle, and to predict the after stall lift by using RANS with turbulent model, ever researches showed that adjust of turbulent model or transition point define can somehow improve the result. For the cognition that RANS approach is limited for the massive separated flow for the highly geometry-specific, "detached", 3-D unsteady configuration might be emphasized for airfoils stall prediction, and then DES method is chosen to try to give a improvement.

Computational Approach

DES method is used in this paper for airfoil stall simulation, and pseudo time step is employed both for Navier-Stokes equations and Spalart-Allmaras turbulence equation. LU-SGS method is used to implicitly discretize the S-A equation.

Governing Equation

The Navier-Stokes equations can be written in integral form as follows:

$$\frac{\partial}{\partial t}\iiint_{\Omega}\vec{w}d\Omega+\iint_{\partial\Omega}\overline{\overline{H}}\cdot\vec{n}ds=\iint_{\partial\Omega}\overline{\overline{H_V}}\cdot\vec{n}ds \quad (1)$$

where $\vec{w}$ is the state vector of conservative variables, $\overline{\overline{H}}$ and $\overline{\overline{H}}_V$ are inviscid and viscous fluxes, respectively. Discretized with the finite volume method, these equations take the following form:

$$\frac{d}{dt}\vec{w}_{ij}^{n+1}+\vec{R}(\vec{w}_{ij}^{n+1})=0 \quad (2)$$

The dual time stepping method[9] is applied to this equation for unsteady simulation, where the fully implicit second-order time integration scheme is used for physical time. This leads to a system of ordinary differential equations as follows:

$$\frac{d}{d\tau}\vec{w}_{ij}^{n+1}+\vec{R}^{*}(\vec{w}_{ij}^{n+1})=0 \quad (3)$$

$$\vec{R}^{*}(\vec{w}_{ij}^{n+1})=\frac{3\vec{w}_{ij}^{n+1}-4\vec{w}_{ij}^{n}+\vec{w}_{ij}^{n-1}}{2\Delta t}+\vec{R}(\vec{w}_{ij}^{n+1})=0 \quad (4)$$

The 5-stage Runge-Kutta method is then applied to integrate Eq. (3) in the pseudo time. The local time stepping, and the artificial viscosity method are employed to accelerate the convergence to the steady state solution.

Spalart-Allmaras Model

The Spalart-Allmaras one equation model solves a partial differential equation for variable υ which is related to turbulent viscosity.

$$\frac{D\tilde{\upsilon}}{Dt}=c_{b1}[1-f_{t2}]\tilde{S}\tilde{\upsilon}-\left[c_{w1}f_w-\frac{c_{b1}}{\kappa^2}f_{t2}\right]\left[\frac{\upsilon}{d}\right]^2+\frac{1}{\sigma}\left[\nabla\cdot((\upsilon+\tilde{\upsilon})\nabla\tilde{\upsilon})+c_{b2}(\nabla\tilde{\upsilon})^2\right]+f_{t1}\Delta U^2 \quad (5)$$

where

$$\upsilon_t=\tilde{\upsilon}f_{v1},\quad f_{v1}=\frac{\chi^3}{\chi^3+c_{v1}^3},\quad \chi\equiv\frac{\tilde{\upsilon}}{\upsilon}$$

υ is the molecular viscosity. The right hand side of Eq.1 composed of production, destruction, and diffusion terms. The parameter included in the production term is expressed as

$$\tilde{S}\equiv S+\frac{\tilde{\upsilon}}{\kappa^2d^2}f_{v2},\quad f_{v2}=1-\frac{\chi}{1+\chi f_{v1}}$$

Here S is the magnitude of vorticity, and d is the distance to the closest wall.

The function f_w is

$$f_w=g\left[\frac{1+c_{w3}^6}{g^6+c_{w3}^6}\right]^{1/6},$$

$$g=r+c_{w2}\left(r^6-r\right),\quad r\equiv\frac{\tilde{\upsilon}}{\tilde{S}\kappa^2d^2}$$

$\upsilon=0$ at the wall and in the free stream. It was also set at 0 at initial. The function f_{t2} is

$$f_{t2}=c_{t3}\exp\left(-c_{t4}\chi^2\right)$$

The constants used in the model are

$c_{b1}=0.1355$, $\sigma=2/3$, $c_{b2}=0.622$, $\kappa=0.41$, $c_{w1}=c_{b1}/\kappa^2+(1+c_{b2})/\sigma$, $c_{w2}=0.3$, $c_{w3}=2$, $c_{v1}=7.1, c_{t1}=1, c_{t2}=2, c_{t3}=1.1, c_{t4}=2$

Detached-Eddy Simulation

The DES formulation is based on a modification to the Spalart-Allmaras RANS model such that the model reduces to its RANS formulation near a solid surface and to a subgrid model away from the wall. It takes advantage of both RANS model in the thin shear layer and the power of LES to resolve geometry dependent and three dimensional eddies.

The DES formulation is obtained by replacing the distance to the nearest wall, d, by $\tilde{d}$, where $\tilde{d}$ is defined as,

$$\tilde{d}\equiv\min(d,C_{DES}\Delta) \quad (6)$$

In the current study, Δ is the largest one among the distances between a cell and it's neighbors. In the current calculation, $C_{DES}=0.65$. and with C-H type grid, flow field was separated into two parts by length scale, as shown in Fig.1.

Calculation of S-A equation

The last term on the right hand side of Eq.5 provides a transition from laminar to turbulent. As the trip term was turned off here in this study, Eq.5 can be rewritten simply:

$$\frac{\partial}{\partial t}\rho\tilde{\upsilon} + \partial_k(\rho\tilde{\upsilon}u_k) = \frac{1}{\sigma}\partial_k[(\rho\upsilon + \rho(1+C_{b2})\tilde{\upsilon})\partial_k\tilde{\upsilon}] - \tilde{\upsilon}\frac{C_{b2}}{\sigma}\partial_k[\rho\partial_k\tilde{\upsilon}] + A_1\tilde{\upsilon} + A_2\tilde{\upsilon}^2 \quad (7)$$

Discretized by the finite volume method, it becomes:

$$\rho\Omega_i\frac{\partial\tilde{\upsilon}_i}{\partial t} = -\sum_\sigma S_\sigma\rho_\sigma\left(u^+_{n,i}\tilde{\upsilon}_i + u^+_{n,\sigma(i)}\tilde{\upsilon}_{\sigma(i)}\right) + \frac{1}{\sigma}\sum_\sigma S_\sigma[\rho_\sigma\upsilon_\sigma + \rho_\sigma(1+C_{b2})\tilde{\upsilon}_\sigma](\partial_k\tilde{\upsilon}_i)_\sigma - \tilde{\upsilon}_i\frac{C_{b2}}{\sigma}\sum_\sigma S_\sigma\rho_\sigma(\partial_n\tilde{\upsilon})_\sigma + \left(A_1\tilde{\upsilon}_i + A_2\tilde{\upsilon}_i^2\right)\Omega_i \quad (8)$$

where

Ω_i cell volume

σ neighbor cell

S_σ cell interface area

n outward normal to cell interface

$u^+ = 0.5(u+|u|)$

$u^- = 0.5(u-|u|)$

Using an implicit time scheme, this equation becomes:

$$\frac{\rho\Omega_i}{\Delta t}\Delta\tilde{\upsilon}_i = -\sum_\sigma S_\sigma\rho_\sigma\left(u^+_{n,i}\tilde{\upsilon}_i^{n+1} + u^-_{n,\sigma(i)}\tilde{\upsilon}_{\sigma(i)}^{n+1}\right) + \sum S_\sigma\Gamma_{dis,\sigma}(\partial_n\tilde{\upsilon})_\sigma^{n+1} + \left(A_1\tilde{\upsilon}^* + A_2(\tilde{\upsilon}^*)^2\right)\Omega_i \quad (9)$$

where

$$\Gamma_{dis,\sigma} = \frac{1}{\sigma}[\rho_\sigma\upsilon_\sigma + \rho_\sigma(1+C_{b2})\tilde{\upsilon}_\sigma - \tilde{\upsilon}_i\rho_\sigma C_{b2}]$$

$$\Delta\tilde{\upsilon}_i = \tilde{\upsilon}_i^{n+1} - \tilde{\upsilon}_i^n$$

$$* = \begin{cases} n, & if\ A_1(or\ A_2) > 0 \\ n+1, & if\ A_1(or\ A_2) < 0 \end{cases}$$

Linearizing the equation along with a pseudo time technique, we have:

$$\rho\Omega_i\frac{\tilde{\upsilon}_i^{n+1,s+1} - \tilde{\upsilon}_i^{n+1,s}}{\Delta\tau} = -\frac{\rho\Omega_i}{\Delta}\left(\tilde{\upsilon}_i^{n+1,s+1} - \tilde{\upsilon}_i^{n+1,s}\right) - \frac{\rho\Omega_i}{\Delta t}\left(\tilde{\upsilon}_i^{n+1,s+1} - \tilde{\upsilon}_i^{n+1,s}\right) + \mathrm{Re}\,s^{n+1,s} - \sum_\sigma S_\sigma\rho_\sigma\left(u^+_{n,i}\delta^s\tilde{\upsilon}_i + u^-_{n,\sigma(i)}\delta\tilde{\upsilon}_{\sigma(i)}\right) + \sum_\sigma S_\sigma\Gamma_{dis,\sigma}\frac{1}{h_\sigma}\left(\delta^s\tilde{\upsilon}_{\sigma(i)} - \delta^s\upsilon_i\right) + \left(A_1 + 2\tilde{\upsilon}_i^{n+1,s}A_2\right)\delta^s\tilde{\upsilon}_i\cdot\Omega_i \quad (10)$$

where

s inner iteration time step

$\delta^s\tilde{\upsilon}_i = \tilde{\upsilon}_i^{n+1,s+1} - \tilde{\upsilon}_i^{n+1,s}$

Since, values at step s are given in inner iterate, the equation becomes linearized equation about $\delta^s\tilde{\upsilon}_i$ which contains unknown variables in neighbor cells, as follows:

$$Coef_1\cdot\delta^s\tilde{\upsilon}_i = \frac{\rho\Omega_i}{\Delta t}\left(\tilde{\upsilon}_i^{n+1,s} - \tilde{\upsilon}_i^n\right) + \mathrm{Re}\,s^{n+1,s} - \sum_\sigma Coef_2\delta^s\tilde{\upsilon}_{\sigma(i)} \quad (11)$$

The LU-SGS method is employed to solve this equation:

$$Coef_1\cdot\delta^s\tilde{\upsilon}^* = R^s - \sum_{\sigma:\ \sigma(i)<i} Coef_2\delta^s\tilde{\upsilon}_{\sigma(i)}$$
$$Coef_1\cdot\delta^s\tilde{\upsilon} = Coef_1\cdot\delta^s\tilde{\upsilon}^* - \sum_{\sigma:\ \sigma(i)>i} Coef_2\delta^s\tilde{\upsilon}_{\sigma(i)} \quad (12)$$

Results

The following three airfoils[10] with different types of stall have been selected in this study.

1. NACA63_3-018 with trailing edge stall
2. NACA63_1-012 with leading edge stall
3. NACA64A-006 with thin airfoil stall

The present calculation is performed for a Reynolds number of 5.8E10^6 and a Mach number of 0.3. The grid used for 3-D flow field is shown in Fig.2

When the flow is separated, and be 3-D and unsteady, the effects of physical time step and inner iterate time step, grid density, are important to make clear for current simulation. As it special character of flow field near stall, the third aerofoil NACA64A-006 is chosen as an example.

Average lift

In current calculation, the free stream in non-dimensionless are as follow:

$V_\infty = 0.355$

$C = 1.0$

$T_{character} = C/V_\infty = 2.82$

From Fig.3, we can see that the average lift cannot appear a convergent property until $T > 10\times T_{character}$.

To give the lift for unsteady case, we integrate the lift from beginning and averaged it, if the value get a converge value, we cognisance it as the final results, as shown in Fig.3.

Time step accuracy

Two time steps, Δt=0.1 (3.5% of the chord passing time) and Δt=0.05 (1.8% of the chord passing time), are chosen under 8° and 11° attack angles that are before stall and after stall especially. As shown in Fig.4 and 5, the lift histories by simulation are almost same at 8° degree. For 11° degree, lift history are not overlapped, but consider the average lift, drag and moment, no marked difference are observed.

Table 1 the effect of time step

AoA=8°	CL	CD	CM
EXP	0.76	0.098	-0.03
△t=0.1	0.604	0.085	-0.047
△t=0.05	0.606	0.086	-0.050
AoA=11°			
EXP	0.81	0.18	-0.11
△t=0.1	0.783	0.169	-0.121
△t=0.05	0.763	0.087	-0.056

From the calculation we can see that, △t near the value $\Delta * C/V_{\infty}$ is acceptable for the unsteady simulation of airfoils, which is coincide with the advice of Spalart,P.R.

Inner iterate steps

In present research work, explicit local time stepping method is used for inner iterate between two physical times. To show the effect of inner time steps, three different value are chose: 2,20,40. The lift histories are shown as Fig.6, the calculation are all began from uniform flow field initial condition, and after inner iterate time steps large than 20, even the foremost lift history are not coincide, it trend to accord as time increase. 20 inner time steps are used in present work.

Grid density in Span

Since DES combines the property of LES, the grid density acts an important effect. We increase the grid density along span because the grid size in span directly affect separation between RANS region and LES region (we define the length scale as the smaller one of distance from wall and grid size, as stated before).

Two different grid density in span are considered: △z=0.04, and △z=0.02. The lift history at AoA=7° and AoA=8° are showed as shown in Fig.7 and 8.

It should be noticed that at 7°, period phenomena are not changed hence no average change appeared, but for 8° degree the lift history are completely changed. Seeing about the force in this case

Table 2 the effect of grid density

AoA=8°	CL	CD	CM
EXP	0.76	0.098	-0.03
△z=0.04	0.604	0.085	-0.047
△z=0.02	0.651	0.095	-0.070

We can see that the lift and drag are much more close to the experiment data.

Compare with experiment

The case of NACA64A-006

In this type of airfoil, as attack angle increases, a separated bubble first appears on the upper surface near the leading edge. The lift increases almost linearly for small attack angles. The first non-linearity in the lift curve appears at $\alpha = 5.27°$, as seen in Fig.12, which is due to a bubble produced near the leading edge (see Figs. 9(a) and 9(b)).

A important phenomena should be notice from the lift history after bubble appear till stall, as shown in Fig.10

Between 6° to 11°, there exit a case whose flow field appear clearly period phenomena, at 6° degree, flow field is steady and 2-D, at 7° degree, flow field become unsteady and period phenomena exist, this phenomena become disappear from 8°, and flow field show no disciplinarian after this attack angle.

Checking flow field at 8° degree at different time point found that large bubble over upper surface; small bubble follow with reattach and separation again; totally separated over upper surface are appeared periodically as time variety. As shown in Fig.11.

Lift curve are shown in Fig.12, it is found that much more careful should be taken near the stall angle, especially just before the stall because of the bubble break down.

The case of $NACA63_1$-012

In this airfoil, as attack angle increases, the flow is suddenly separated from the leading edge, which covers all over the upper surface of airfoil, leading to lift loss after stall. The flow field is shown in Fig.13 (a) for before-stall case and Fig.13 (b) for after-stall case. By using RANS with B-L turbulence model, we can only catch the stall angle, but the lift after stall can't be simulated [11]. However, in the DES method, not only stall angle can be determined accurately, but also, large separated flow after stall can be simulated in detached region. The variation of lift with attack angle is shown in Fig.14.

The case of $NACA63_3$-018

The lift loss in this case is caused by flow separation near the trailing edge, which extends rather slowly toward the upstream as attack angle increases. This process is shown in Figs.15 (a) and 15 (b). No obvious differences are observed between the RANS and DES methods, as shown in Fig.16. This means that, for slightly separated flows, use of the B-L turbulence model can provide reliable results.

Conclusion

In this study, the properties of three different stall types of airfoil were simulated.

For the small separated flow field, such as $NACA63_3$-018 at the attack angle just after

maximum lift, DES get good result for lift estimate, anyway, RANS method can also get the same result for the local upper surface separation.

For the massive separated flow, DES method showed much more reasonable results than RANS method, as shown by NACA63_1-012.

Present calculation meet some difficult at the case of thin airfoil stall type, when the bubble begin unstable and appear period variation. After fully separated, present calculation again get reasonable results, as shown in example NACA64A-006. For this case, span width, time step or others calculation condition may affect the numerical result, much more research need to concentrate to this point.

References

[1] M. Strelets, St. Peterburg, "Detached Eddy Simulation of Massively Separated Flows", AIAA 2001-0879.

[2] Spalart,P.R., "Trends in Turbulence Treatmens", AIAA paper 2000-2306

[3] Spalart,P.R., Jou,W.-H., Strelets,M., and Allmaras,S.R. Comments on the feasibility of LES for wings, and on a hybrid RANS/LES approach. 1st AFOESR Int. Conf. On DNS/LES, (1997), Ruston,LA. In Advances in DES/LES, C.Liu & Z.Liu Eds., Greyden Press,Columbus,OH.

[4] Morton, S., Forsythe, J.R., Mitchell, A., and Hajek, D., "Des and RANS Simulations of Delta Wing Vortical Flows", AIAA 2002-0587.

[5] James R. Forsythe, Klaus A. Hoffmann, Kyle D. Squires, "Detached-Eddy Simulation with Compressibility Corrections Applied to a Supersonic Axisymmetric Base Flow", AIAA 02-0586.

[6] Squires, K.D., Forsythe, J.R., Morton, S.A., Strang, W.Z., Wurzler, K.E., Tomaro, R.F., Grismer, M.J., and Spalart, P.R., "progress on Detached–Eddy Simulation of Massively Separated Flows" AIAA 2002-1021.

[7] James R. Forsythe, Kyle D. Squires, Kenneth E. Wurtzler, Philippe R. Spalart, "Detached-Eddy Simulation of Fighter Aircraft at High Alpha", AIAA 2002-0591.

[8] "Proceedings of Aerospace Numerical Simulation Symposium 2000", Special Publication of National Aerospace Laboratory, NAL SP-46, ISSN 0289-260X.

[9] Arnone, A., Liou, M.S., and Povinelli, L.A., "Integration of Navier-Stokes Equations Using Dual Time Stepping and a Multigrid Method" AIAA Journal, Vol.33,No.6,June 1995.

[10] George,B. and Donald, E., "Examples of Three Representative Types of Airfoil Section Stall at Low Speed", NACA TN-2502, 1951.

[11] Li Dong, Igor Men'shov, and Yoshiaki Nakamura, "2-D RANS Simulation for Three Different Stall Types", Proceedings of the Thirty-fifth Fluid Dynamics Conference of Japan, Kyoto, Japan, 2003,9.

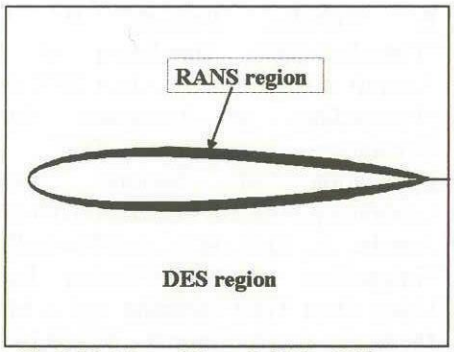

Fig.1 Division of flow-field for DES

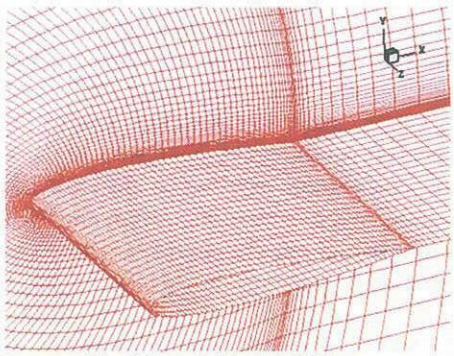

Fig.2 the grid for airfoil

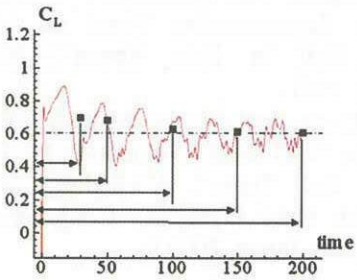

Fig.3 Average lift history

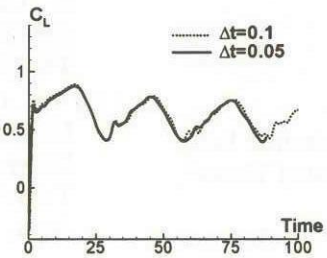

Fig.4 lift history at AoA=8°

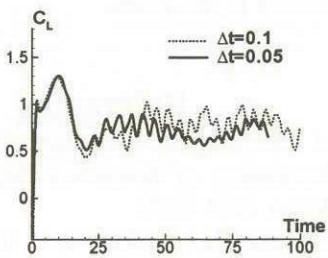

Fig.5 lift history at AoA=11°

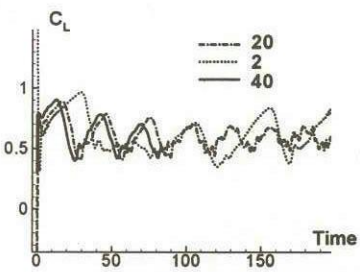

Fig.6 inner iterate steps effect

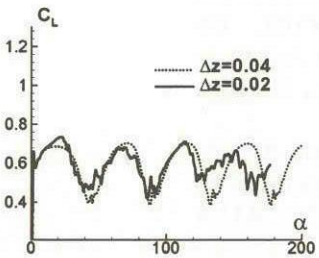

Fig.7 lift history at AoA=7°

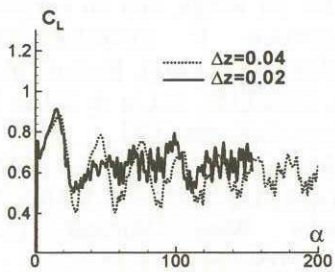

Fig.8 lift history at AoA=8°

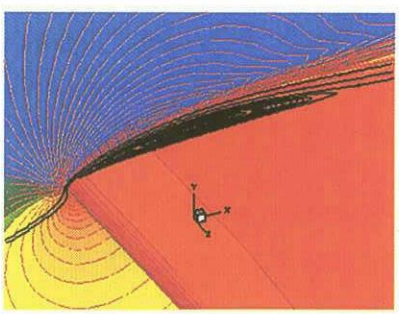

(a) $\alpha = 5.27^{o}$

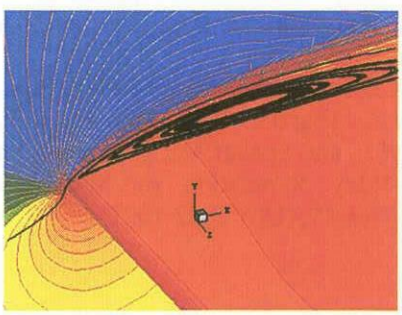

(b) $\alpha = 6^{o}$

Fig.9 Flow field of NACA64A-006

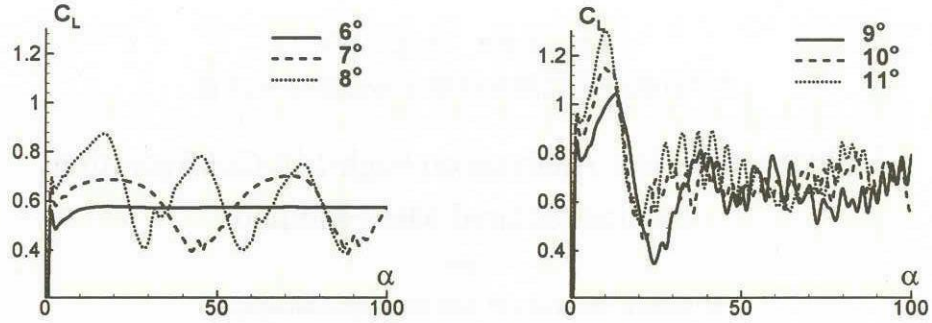

Fig.10 lift history from AoA=7° to AoA=11°

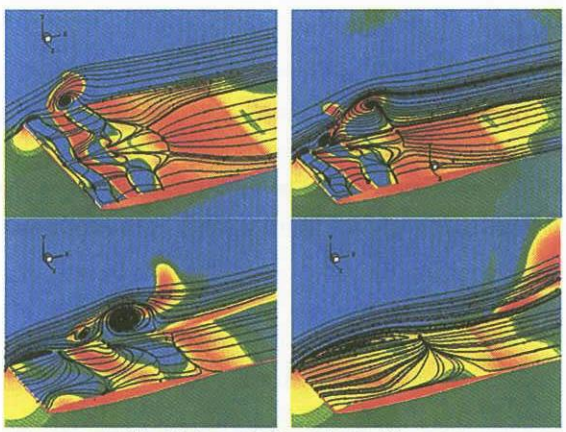

Fig.11 flow field at AoA=8°

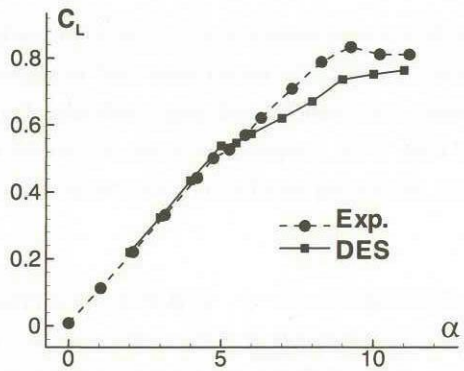

Fig.12 Lift vs. attack angle for NACA64A-006

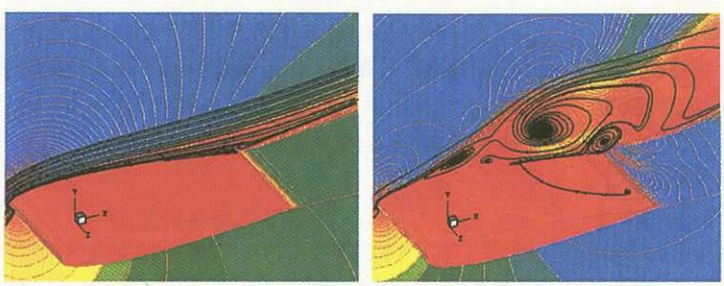

(a) $\alpha = 14^o$ (b) $\alpha = 15^o$

Fig.13 Flow field of $NACA63_1$-012

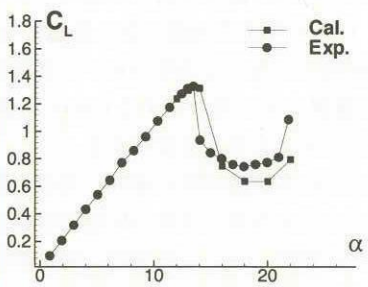

Fig.14 Lift vs. attack angle for $NACA63_1$-012

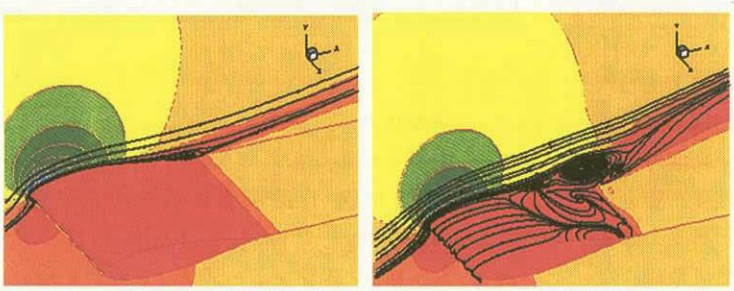

(a) $\alpha = 15^o$ (b) $\alpha = 16^o$

Fig.15 Flow field of $NACA63_3$-018

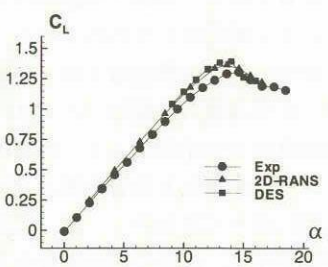

Fig.16 Flow field of $NACA63_3$-018